CHEMISTRY OF MATERIALS
Article

Chem. Mater. **2010,** *22,* 5593–5600 5593
DOI:10.1021/cm101696t

Microcapsules with Tailored Nanostructures by Microphase Separation of Block Copolymers

Jae Won Shim,[†] Shin-Hyun Kim,[†] Seog-Jin Jeon,[†,§] Seung-Man Yang,*[,†] and Gi-Ra Yi*[,‡]

[†]*National Creative Research Initiative Center for Integrated Optofluidic Systems and Department of Chemical and Biomolecular Engineering, KAIST, Daejeon 305-701, Korea, and* [‡]*Department of Industrial Engineering Chemistry, Chungbuk National University, Chungbuk, 361-763 Korea.* [§]*Current address: Material & Device Center, Samsung Advanced Institute of Technology, Yongin 449-712, Korea.*

Received June 17, 2010. Revised Manuscript Received August 29, 2010

Colloidal microcapsules of thin nanoshell membranes were prepared by the evaporation-induced self-assembly of poly(styrene)-block-poly(butadiene)-block-poly(styrene) (SBS) triblock copolymers inside the oil phase of a water-in-oil-in-water (W/O/W) double emulsion, which was prepared via a two-step sequential emulsification process. To see the nanoconfinement effect, the shell thickness was kept very thin and comparable to the feature scale of self-organized nanostructure. By exploiting the density mismatch between the microcapsules and the continuous medium, single-cored microcapsules with thin shells were selectively separated from mixtures of multicored microcapsules or thick-shelled microcapsules. The internal morphology of the membrane could be modulated by controlling the volume fractions of styrene and butadiene blocks, which was achieved simply by adding polystyrene homopolymer of relatively low molecular weight. By varying the amount of homopolymer, various morphologies were produced in the microcapsule membranes, including lamellae, perforated lamellae, and cylindrical and spherical phases. Moreover, the addition of polystyrene homopolymer could be used to control the mechanical characteristics of the microcapsules.

Introduction

Over the past few decades, supramolecular self-assembly has attracted considerable attention in nanofabrication as an alternative to expensive lithographic processes.[1−3] In particular, block copolymer self-assembly has emerged as one of the most promising routes to nanostructures, because it can produce nanopatterns with structural complexity over large areas.[4,5] By varying the block copolymer composition, segment−segment interaction parameters, and degree of polymerization, a variety of morphologies have been obtained and used for the nanopatterning of planar substrates consisting of organic, inorganic, semiconducting, metallic, or biologically relevant materials.[6,7] Recently, the microphase separation of block copolymers has been achieved in nonplanar confining geometries such as cylindrical pores[8] and emulsion droplets.[9,10] Depending on the surface preference and the size of the confining geometry relative to the characteristic length of the microphase, unique and anomalous morphologies have been observed in both experimental and theoretical studies.[11−15]

Meanwhile, encapsulation technologies have long been a topic of interest, because of their wide range of applications in foods, drugs, and cosmetics.[16−19] Emulsion droplets have been used as templates for preparing spherical microparticles to encapsulate active materials. In addition, double-emulsion droplets have been employed to generate microcapsules containing liquid cores,[20−22] in

*Authors to whom correspondence should be addressed. E-mail: smyang@kaist.ac.kr (S.M.Y.), yigira@chungbuk.ac.kr (G.R.Y.).

(1) Ramos, L.; Lubensky, T. C.; Dan, N.; Nelson, P.; Weitz, D. A. *Science* **1999**, *286*, 2325–2328.
(2) Yang, S.-M.; Jang, S. G.; Choi, D.-G.; Kim, S.; Yu, H. K. *Small* **2006**, *2*, 458–475.
(3) Yin, Y.; Lu, Y.; Gates, B.; Xia, Y. *J. Am. Chem. Soc.* **2001**, *123*, 8718–8729.
(4) Bates, F. S. *Science* **1991**, *251*, 898–905.
(5) Lopes, W. A.; Jaeger, H. M. *Nature* **2001**, *414*, 735–738.
(6) Cheng, J. Y.; Ross, C. A.; Smith, H. I.; Thomas, E. L. *Adv. Mater.* **2006**, *18*, 2505–2521.
(7) Wang, Y.; Hong, X.; Liu, B.; Ma, C.; Zhang, C. *Macromolecules* **2008**, *41*, 5799–5808.
(8) Shin, K.; Xiang, H.; Moon, S. I.; Kim, T.; McCarthy, T. J.; Russell, T. P. *Science* **2004**, *306*, 76.
(9) Jeon, S.-J.; Yi, G.-R.; Koo, C. M.; Yang, S.-M. *Macromolecules* **2007**, *40*, 8430–8439.
(10) Yabu, H.; Higuchi, T.; Shimomura, M. *Adv. Mater.* **2005**, *17*, 2062–2065.
(11) Jeon, S.-J.; Yi, G.-R.; Yang, S.-M. *Adv. Mater.* **2008**, *20*, 4103–4108.
(12) Tanaka, T.; Saito, N.; Okubo, M. *Macromolecules* **2009**, *42*, 7423–7429.
(13) Higuchi, T.; Tajima, A.; Motoyoshi, K.; Yabu, H.; Shimonura, M. *Angew. Chem., Int. Ed.* **2008**, *47*, 8044–80146.
(14) Okubo, M.; Saito, N.; Takekoh, R.; Kobayashi, H. *Polymer* **2005**, *46*, 1151–1156.
(15) Pinna, M.; Guo, X.; Zvelindovsky, A. V. *Polymer* **2008**, *49*, 2797–2800.
(16) (a) Dubey, R.; Shami, T. C.; Bhasker Rao, K. U. *Defense Sci. J.* **2009**, *59*, 82–95. (b) Degim, I. T.; Celebi, N. *Curr. Pharm. Des.* **2007**, *13*, 99–117.
(17) Davis, S. S.; Walker, I. M. *Methods Enzymol.* **1987**, *1749*, 51–64.
(18) Tjipto, E.; Cadwell, K. D.; Quinn, J. F.; Johnston, A. P. R.; Abbott, N. L.; Caruso, F. *Nano Lett.* **2006**, *6*, 2243–2248.
(19) Becker, A. L.; Zelikin, A. N.; Johnston, A. P. R.; Caruso, F. *Langmuir* **2009**, *25*, 14079–14085.
(20) Pannacci, N.; Bruus, H.; Bartolo, D.; Etchart, I.; Lockhart, T.; Hennequin, Y. *Phys. Rev. Lett.* **2008**, *101*, 164502.

© 2010 American Chemical Society
Published on Web 09/08/2010

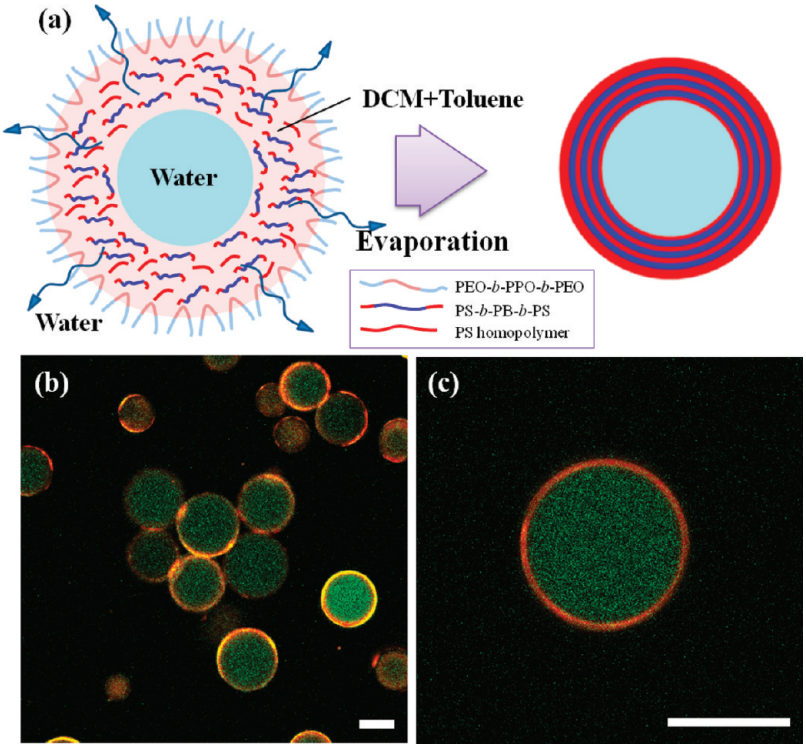

Figure 1. (a) Schematic illustration for preparation of microcapsules with nanostructure, based on microphase separation of block copolymers in the middle phase of the double-emulsion droplets. (b, c) Confocal laser scanning microscopy (CLSM) images of microcapsules encapsulating FITC-labeled dextran, where shells are doped with Nile-Red. The scale bars in panels (b) and (c) are each 20 μm.

which the middle phase of the double emulsion droplets is selectively solidified by polymerization[23−26] or evaporation-induced consolidation.[21,22,27,28] For example, optofluidic encapsulation can be used to confine an aqueous suspension containing a crystalline colloidal array within a spherical membrane through in situ photopolymerization of the middle phase.[26] However, most of the previous microcapsules composed of a solid shell do not have any nanostructures in the membrane. Although a few recent papers reported microcapsules of nanopores or micropores, the regularity of the pores was not good enough to facilitate controlled mass transfer through the membrane.[27,28] On the other hand, amphiphilic block copolymers have been explored in studies of so-called "polymersomes", which show enhanced stability and controlled permeability compared with liposomes.[21,22] However, the bilayered membranes behave like a semipermeable membrane that allows only very small molecules to pass through it.

In the present study, we prepared polymeric microcapsules of nanostructured membrane using symmetric poly(styrene)-*block*-poly(butadiene)-*block*-poly(styrene) (SBS) triblock copolymers, which were confined in the oil phase of water-in-oil-in-water (W/O/W) double-emulsion droplets. The microphase separation of the block copolymer created an ordered nanostructure in the thin membrane of microcapsules, which is potentially useful in the preparation of regular nanopores for controlled mass transfer through a membrane. Here, the shell membranes were made nanoscopically thin, to see the confinement effect on the phase morphology. Because the double-emulsion droplets were prepared by sequential emulsification, their size distribution and the number of cores in each droplet could not be controlled precisely.[29] However, we could separate high-quality microcapsules through a simple separation scheme, based on selective sedimentation after consolidation of the middle phase. In addition, the internal nanoscopic morphology resulting from microphase separation of the block copolymers was investigated by slicing individual microcapsules with an ultramicrotome and examining the internal structure using transmission electron microscopy (TEM) analysis. The nanostructure of the block copolymers inside the microcapsule shells was modulated precisely by adding PS homopolymer (*h*PS) with relatively low molecular weight, and the mechanical properties of the microcapsules varied, depending on the block copolymer composition.

In the subsequent sections, we first described the method for preparing microcapsules with thin block copolymer shells and the selective separation process. We then examined the microphase separation of block copolymers

(21) Shum, H. C.; Kim, J.-W.; Weitz, D. A. *J. Am. Chem. Soc.* **2008**, *130*, 9543–9549.
(22) Hayward, R. C.; Utada, A. S.; Dan, N.; Weitz, D. A. *Langmuir* **2006**, *22*, 4457–4461.
(23) Hennequin, Y.; Pannacci, N.; Torres, C.; T.-Meris, G.; Chapuliot, S.; Bouchaud, E.; Tabeling, P. *Langmuir* **2009**, *25*, 7857–7861.
(24) Nie, Z.; Xu, S.; Seo, M.; Lewis, P. C.; Kumacheva, E. *J. Am. Chem. Soc.* **2005**, *127*, 8058–8063.
(25) Kim, J.-W.; Utada, A. S.; Fernandez-Nieves, A.; Hu, Z.; Weitz, D. A. *Angew. Chem., Int. Ed.* **2007**, *46*, 1819–1822.
(26) Kim, S.-H.; Jeon, S.-J.; Yang, S.-M. . *J. Am. Chem. Soc.* **2008**, *130*, 6040–6046.
(27) Lee, D.; Weitz, D. A. *Adv. Mater.* **2008**, *20*, 3498–3503.
(28) Choi, S.-W.; Zhang, Y.; Xia, Y. *Adv. Funct. Mater.* **2009**, *19*, 2943–2949.
(29) Ikkai, F. *Langmuir* **2008**, *24*, 3412–3416.

confined in the middle phase of double-emulsion droplets. Finally, we discussed the effect of *h*PS on the morphology of the block copolymers as well as the mechanical properties of the microcapsules.

Results and Discussion

In this work, two-step sequential emulsification was used to prepare double-emulsion droplets, which is the only route to the mass production of such droplets at low cost. In the first emulsification, water-in-oil (W/O) droplets were prepared in which the oil phase was comprised of SBS triblock copolymers and *h*PS in a mixture of dichloromethane (DCM) and toluene. In subsequent emulsification, the W/O emulsion droplets were emulsified into aqueous solution containing oil-stabilizing surfactant using a homogenizer, resulting in a polydisperse mixture of simple (oil-in-water), single-cored double, and multicored double emulsion droplets. Thus, by evaporation of volatile organic solvents, those emulsions were solidified, which produced polymeric microspheres, or microcapsules with single cores or multicores. To separate the single-cored microcapsules from the mixture, we used a selective sedimentation process that separated microcapsules on the basis of their average density. When the density ratio ($\gamma = \rho_{capsule}/\rho_{continuous}$) of microcapsules to continuous phase is >1, microcapsules should settle slowly. The density of microcapsules can be determined by the following equation:

$$\rho_{capsule} = \phi_{core}\rho_{core} + \phi_{shell}\rho_{shell}$$

where ϕ_{core} and ϕ_{shell} are volume fractions of core and shell inside microcapsules, respectively. When the densities of the core (ρ_{core}), continuous phase ($\rho_{continuous}$), and shell (ρ_{shell}) are in the order $\rho_{core} > \rho_{continuous} > \rho_{shell}$, the single-cored microcapsules with shells can be settled in a case when a shell volume is sufficiently small enough to make the average density of the capsules ($\rho_{capsule}$) higher than $\rho_{continuous}$. Otherwise, polymeric capsules or particles should be creamed up. From a simple consideration of average density, the ratio of critical shell thickness to microcapsule radius can be determined for $\gamma > 1$:

$$\frac{t_{critical}}{R} = \left(\frac{\rho_{core} - \rho_{shell}}{\rho_{continuous} - \rho_{shell}}\right)^{1/3} - 1 \qquad (1)$$

where ρ_{shell} is determined by the fraction of polystyrene (PS) and polybutadiene (PB) chains in the polymer blend.

Therefore, through the sedimentation process, we could obtain microcapsules with thin shells from bulk mixtures without the need for complex and inefficient procedures such as sieving. For instance, when microcapsules have thin shells with lower density but cores with higher density than the continuous phase, they settle slowly. By contrast, multicored microcapsules or thick-shelled capsules float on top of the continuous phase. Therefore, we can selectively separate single-cored microcapsules with thin shells by controlling the density of the continuous phase.

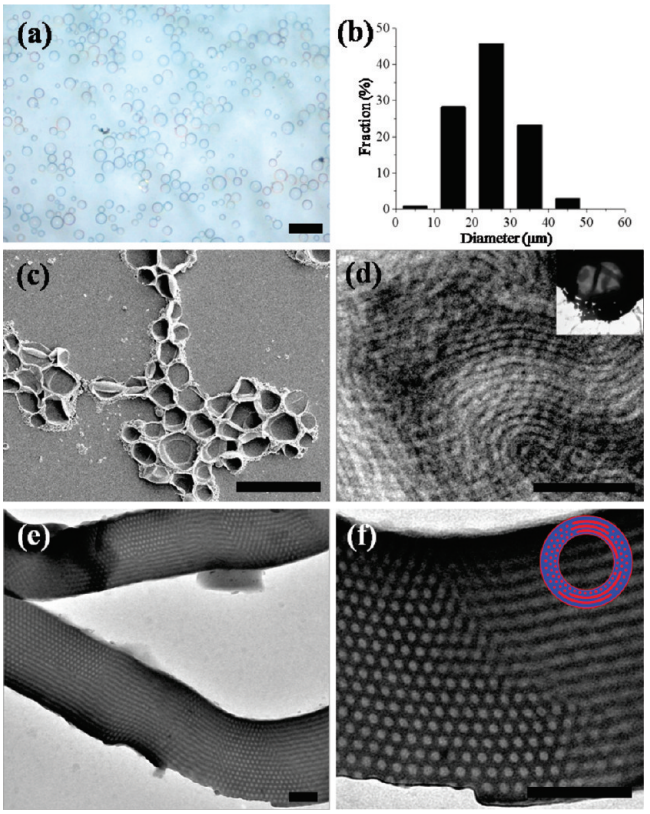

Figure 2. (a) Optical microscopy image of microcapsules with $f_s = 0.31$ dispersed in water. (b) Size distribution of the microcapsules based on panel (a). (c) SEM images of dried microcapsules with $f_s = 0.31$. All capsules were completely deflated during drying due to high flexibility of the membrane. (d) TEM images taken at the central part of deflated microcapsules where two line patterns from two membranes were overlapped. The inset in panel (d) is a TEM image of a deflated capsule at low magnification. (e, f) TEM images showing a cross section of a shell membrane of the microcapsule. The inset of panel (f) is a schematic of the prepared microcapsules with cylindrical microphase in shell. The scale bars in panels (a) and (c) and panels (d, e, f) are 100 μm and 200 nm, respectively.

To confirm the successful separation of microcapsules, and to identify their core−shell structure, we dissolved fluorescein isothiocyanate (FITC)-labeled dextran and Nile-Red dye molecules in the core and middle phases, respectively. After complete evaporation of the middle phase and separation, the microcapsules were observed by confocal laser scanning microscopy (CLSM), in which the aqueous dextran cores are labeled with FITC and the polymeric shells are doped with Nile-Red (see Figures 1b and 1c). The images show uniform thickness of the membrane, which contributes to the uniform oil layer in double-emulsion droplets. A large resistance of lubrication film, highly thin oil layer, against a gravitational force on core droplet makes relatively concentric core and shell droplets. Inside the thin shells of the microcapsules, the triblock copolymers self-organized into ordered nanostructures by thermal annealing at 95 °C, as schematically depicted in Figure 1a. The interface between the middle and continuous phases in each double-emulsion droplet is stabilized with the block copolymer surfactant poly(ethylene oxide)-block-poly(propylene oxide)-block-poly(ethylene oxide) (PEO-*b*-PPO-*b*-PEO, Pluronic F108, BASF).

Microcapsules with a Cylindrical PS Phase. Block copolymers inside the thin-shelled microcapsules can form various nanoscale morphologies through microphase separation, depending on the volume fraction of the styrene (or butadiene) block. In this study, we used blends of block copolymer with *h*PS to control the volume fraction instead of block copolymers with different molecular weight ratios.[9,11] As a starting point, we prepared microcapsules composed of SBS triblock copolymers with a PS weight fraction (f_s) of 0.31. Because the block copolymer of PB (ρ_{PB} = 0.892 g/cm^3) and PS (ρ_{PS} = 1.05 g/cm^3) with f_s = 0.31 has an average density of 0.941 g/cm^3, we used a 3.85 wt % aqueous solution of gelatin (ρ_{core} = 1.013 g/cm^3) as the core liquid and 0.1 wt % aqueous solution of PEO-*b*-PPO-*b*-PEO ($\rho_{continuous}$ = 1.0003 g/cm^3) as the outer continuous medium, in which microcapsules with thin shells ($t_{critical} < 1$ μm) were successfully separated by spontaneous sedimentation. The sequential emulsification and subsequent evaporation of the volatile organic phase produced a mixture of various types of microspheres; this is demonstrated in the inverted optical microscopy image in Figure S1 in the Supporting Information, in which the transparent microspheres are single-cored microcapsules and the opaque or relatively small spheres are multicolored microcapsules or microparticles. Notably, the transparent microcapsules are larger than the other microspheres. The size distributions of the transparent and opaque spheres are shown in Figure S1b in the Supporting Information.

Through an acceleration of the sedimentation-induced separation by centrifugation at 8500 rpm for 10 min, we could collect the microcapsules from the mixture as shown in Figure 2a. Many transparent microcapsules show color at their edges under reflection-mode optical microscopy, because of optical interference induced by the thin membrane.[29] The size distribution of the microcapsules is shown in Figure 2b, where the microcapsule average diameter and coefficient of variation (CV) are 25 μm and 0.328, respectively. According to eq 1, we can estimate $t_{critical}/R$ as 0.067 and, therefore, the separated microcapsules will have a thin shell with a thickness of $<$ 837.5 nm.

The microcapsules were completely deflated during drying of the aqueous core, as shown in the SEM image in Figure 1c. The Young's modulus of the PB phase is as low as 1.6 MPa, and its flexural yield strength is not measurable, because of its intrinsic rubbery property. PS has a Young's modulus of 3.1 GPa and a flexural yield strength of 70 MPa.[30] Therefore, when the majority of the SBS block copolymer is PB ($f_s < 0.5$), its membrane will be highly flexible. In systems with such block copolymers, the pressure decrease in the core during evaporation induces total deflation, resulting in two stacked block copolymer shells. The internal morphology of the shells can be observed normal to the surface using TEM (Figure 2d). As shown in the low-magnification image in the inset of Figure 2d, the central part of the deflated

(30) http://www.matweb.com/reference/flexuralstrength.aspx (accessed April 22, 2010).

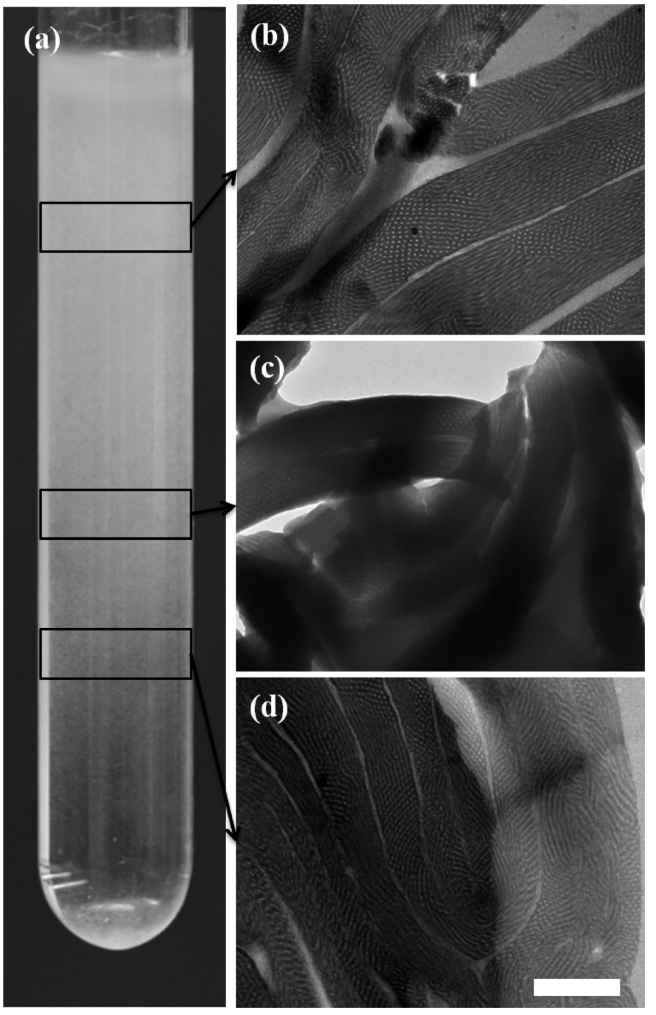

Figure 3. (a) Optical image showing continuous separation of microcapsules depending on the average density through centrifugation in density gradient medium. (b, c, d) Cross-sectional TEM images of microcapsules obtained from regions (denoted by arrows). The magnification scales are the same for all TEM images, and the scale bar in panel (d) is 500 nm.

microcapsule is relatively transparent, because of the small thickness of the membrane, and overlapping line patterns with two different directions can be discerned. To elucidate the morphology, we prepared ultrathin pieces containing a cross section of the membrane. The TEM images in Figures 2e and 2f show the morphology of the microphase clearly, where PB is selectively stained by OsO_4 to increase the contrast. The magnified TEM image in Figure 2f exhibits hexagonal and parallel arrays of PS cylinders in a continuous PB domain in the left and right sides of the image, respectively. The PS cylinders are predominantly aligned parallel to the inner and outer surfaces of the microcapsules. Therefore, the line patterns in Figure 2d can be understood as arising from overlapping cylindrical phases in the top and bottom membranes. The localization of the PS phase at the two interfaces of the block copolymer shells (inside and outside) can be attributed to the higher affinity of the PS than the PB blocks for the interface between water and the organic solvent, as described in a previous report.[11] However, we could not explore this hypothesis experimentally, because

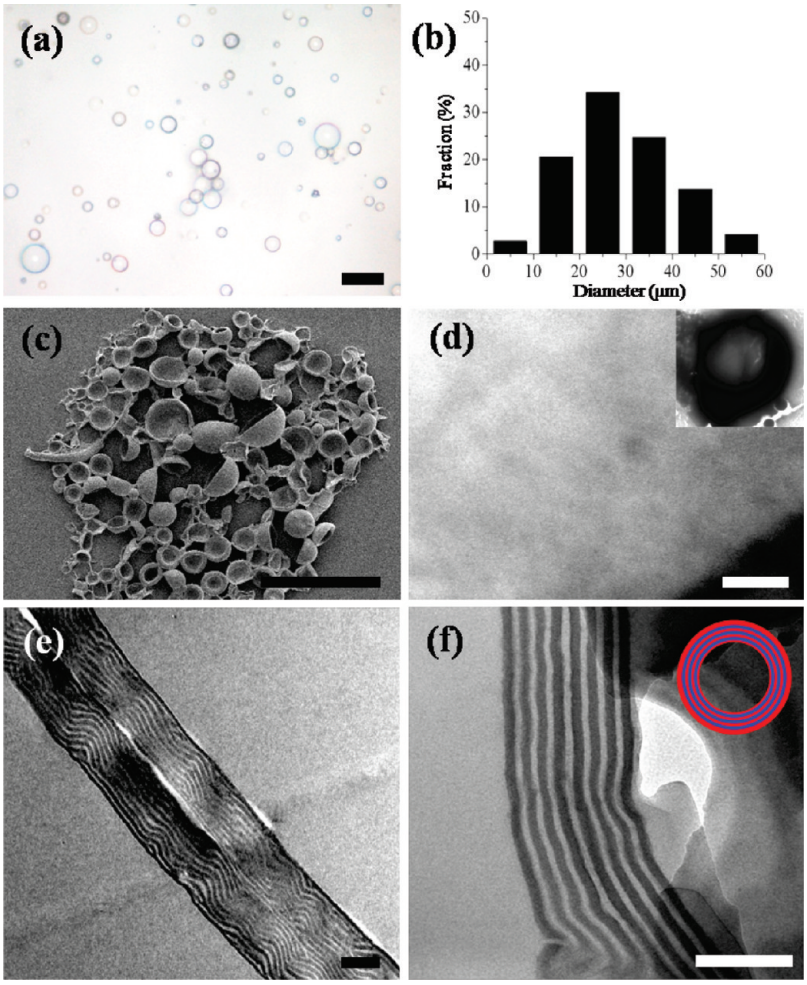

Figure 4. (a) Optical microscope image of microcapsules with $f_s = 0.50$ dispersed in water. (b) Size distribution of the microcapsules based on panel (a). (c) SEM images of dried microcapsules with $f_s = 0.50$. All capsules were deflated during drying. (d) TEM images taken at the central part of deflated microcapsules where distinctive nanostructures were not observed. The inset in panel (d) is a TEM image of a deflated capsule at low magnification. (e, f) TEM images showing cross sections of the shell membrane of a microcapsule. The inset of panel (f) is a schematic of the prepared microcapsules with a lamellae microphase in the shell. The scale bars in panels (a, c) and (d, e, f) are 100 μm and 200 nm, respectively.

of the low contrast between PS and the epoxy matrix in the TEM images, as shown in Figure 2e or 2f. The inset of Figure 2f shows a schematic illustration of a microcapsule comprised of a cylindrical PS phase embedded in a continuous PB domain with a thin PS layer at both the inner and outer interfaces.

The thickness of the shell membrane showed a size distribution because we collected all microcapsules with shell thicknesses smaller than ~1 μm. To fractionate the microcapsules according to shell thickness, we employed a density gradient of the continuous phase, which is prepared using a device that was composed of two connected jars.[31] Using distilled water in one jar and a 5 wt % aqueous solution of polysaccharide (Ficoll PM 400) in another jar, we created a concentration gradient of polysaccharide through the glass tube connecting the jars, resulting in a density gradient of 1−1.017 g/cm^3. We then centrifuged the tube using a swing bucket at an acceleration of 4500 g for 20 min, after careful loading of an aqueous suspension of microcapsules on top. The microcapsules settled until they reached the level at which their density matched that of the continuous phase. Because the average microcapsule density has contributions from a high-density core (1.013 g/cm^3) and low-density shell (0.941 g/cm^3), microcapsules with thinner membranes settled to lower levels in the tube. Figure 3a shows a glass tube containing microcapsules dispersed in aqueous solution with a density gradient. Figures 3b−d show cross-sectional TEM images of microcapsules obtained from the positions denoted in Figure 3a. The data demonstrate the decrease in shell thickness with increasing sedimentation distance. In addition, the thickness distribution of the capsules membrane taken from a particular range of sedimentation distances, as shown in Figures 3b−d, was narrowed in comparison with that before fractionation. The average thicknesses of the membranes shown in Figures 3b, 3c, and 3d are 330, 260, and 180 nm, respectively. On the other hand, the membrane in each microcapsule showed uniform thickness, which is attributed to concentric core and shell droplets. Because of the large resistance of lubrication film for highly thin oil layer,

(31) (a) Cho, Y. S.; Yi, G.-R.; Kim, S.-H.; Pine, D. J.; Yang, S. M. *Chem. Mater*. **2005**, *17*, 5006–5013. (b) Manoharan, V. N; Elsesser, M. T.; Pine, D. J. *Science* **2003**, *301*, 483–487.

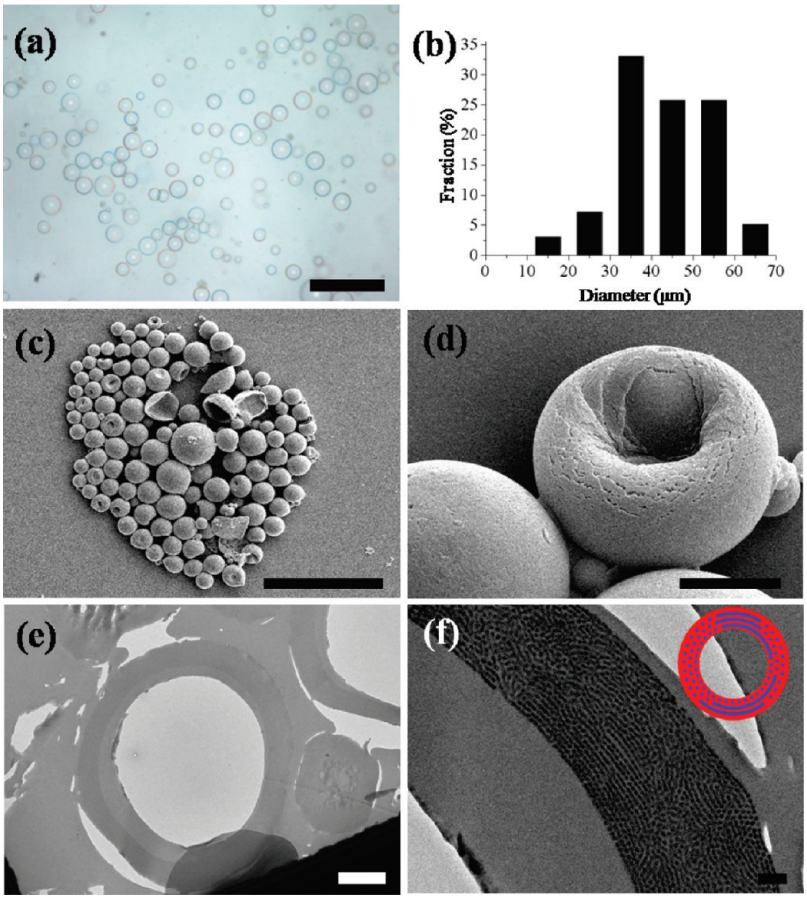

Figure 5. (a) Optical microscopy image of microcapsules with $f_s = 0.70$ dispersed in water. (b) Size distribution of the microcapsules based on panel (a). (c) SEM image of dried microcapsules with $f_s = 0.70$. Most of the microcapsules kept a spherical shape, even after drying, because of enhanced rigidity, although a few microcapsules were indented. (d) Magnified SEM image of an indented microcapsule. (e) TEM image showing the cross section of a shell membrane where a continuous spherical loop was observed. (f) Magnified TEM image showing cylindrical PB phases in the shell. Inset of panel (f) is a schematic of the prepared microcapsules. The scale bars in panels (a, c), (d), (e), and (f) are 00, 5, 2 μm, and 200 nm, respectively.

a core droplet can maintain a uniform thickness of the oil layer against a gravitational force.

Microcapsules of the Lamellae Phase. The effect of the presence of *h*PS on the internal microphase morphology of the block copolymers was explored by controlling the mixing ratio of *h*PS and SBS triblock copolymers. The molecular weight of *h*PS was carefully chosen to be 2400 g/mol, which is much smaller than that of the SBS triblock copolymers (~110 000 g/mol). In the wet-brush regime,[9] *h*PS with a small molecular weight tends to penetrate into the polymeric brushes of PS blocks at microdomain interfaces. The penetrated *h*PS swells the PS blocks and thus increases the effective volume of the PS blocks.[32] Therefore, the addition of *h*PS should induce a similar effect on microphase separation to increase of the PS chain length in the block copolymer. When the weight fraction of PS increased from 0.31 to 0.50 by adding *h*PS, the shell density also increased to 0.971 g/cm^3, which is comparable to the density of the aqueous gelatin core. Therefore, we used a 10 w/v% Ficoll solution for the aqueous core phase (1.04 g/cm^3), to enhance the density contrast. Figures 4a and 4b show microcapsules with thin membranes selectively collected from a mixture prepared by sequential emulsification and evaporation of the middle phase and their size distribution, respectively, where the average diameter was 29 μm and the CV was 0.429. During drying, the microcapsules were deflated as shown in Figure 4c. However, the shape of the deflated capsules differed from that of the capsules with $f_s = 0.31$ in Figure 2c. The increased PS fraction in the shell makes the capsules slightly less rubbery, although the membrane is still flexible. When we observed the central part of the deflated capsules with TEM, no significant nanodomains were observed (Figure 4d). On the other hand, an alternating line pattern appeared in the cross section of the membrane (Figures 4e and 4f), which corresponds to a lamellae phase. Because the layers in the lamellae phase were formed parallel with the wall, like onion rings, the TEM image taken normal to the surface does not display any morphologic features. Here, the innermost and outermost layers were PS, similar to the capsules with $f_s = 0.31$. Schematics of the microcapsules with the lamellae phase are shown in the inset of Figure 4f.

Microcapsules of Cylindrical PB Phase. When the weight fraction of the PS chains exceeds 0.5, the internal microphases are inverted to PB nanodomains embedded in a continuous PS phase. When the weight fraction of PS chains is 0.70, the shell density becomes 1.003 g/cm^3.

(32) Hashimoto, H.; Fujimara, M.; Hashimoto, T.; Kawai, H. *Macromolecules* **1981**, *14*, 844–851.

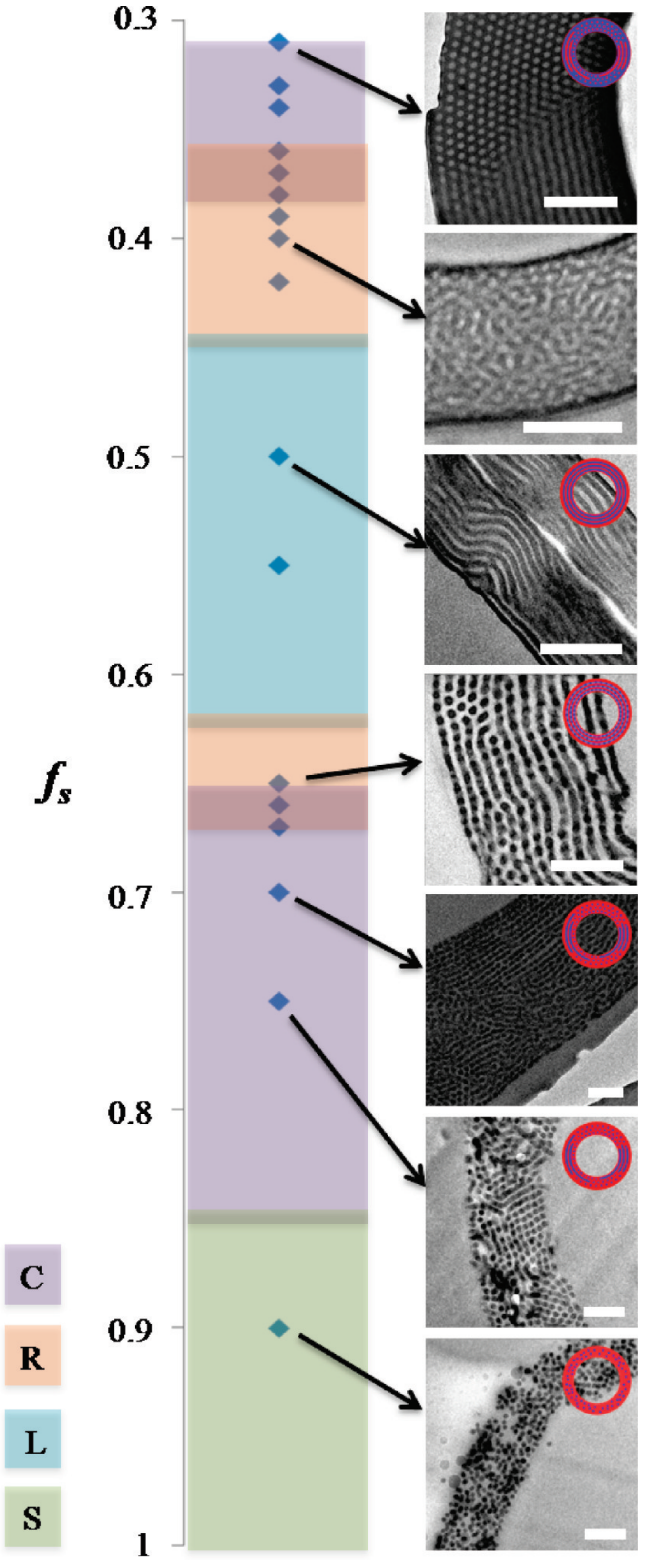

Figure 6. TEM images and diagram displaying microphase transition, according to the weight fraction of PS in blends of SBS triblock copolymer and PS homopolymer. Inset of TEM images shows a schematic of the prepared microcapsules where the second TEM image does not have a scheme because of the absence of a regular nanostructure. The capsules in the images (first to last) have f_s values of 0.31, 0.40, 0.50, 0.66, 0.70, 0.75, and 0.90. The scale bars are 200 nm in all of the TEM images.

Using a 20 w/v% aqueous Ficoll solution as the core (1.08 g/cm^3) and an aqueous mixture of 10 wt % Ficoll and 0.1 wt % PEO-*b*-PPO-*b*-PEO triblock copolymer surfactant (1.04 g/cm^3) as the continuous phase, we prepared microcapsules with $f_s = 0.70$, as shown in Figure 5a. The size distribution of the capsules is described in Figure 5b, where the average diameter of the capsules and CV are 43.5 μm and 0.286, respectively. Because PS, which is characterized by a high Young's modulus and finite flexural yield strength, forms the continuous phase in the shell, most of the microcapsules maintained a spherical shape even during drying of the core phase, although a few microcapsules with thin membranes were indented (Figure 5c). The high magnification image of an indented microcapsule shown in Figure 5d discloses that the membrane in the highly folded region exhibits short cracks, because of the brittleness of the membrane; such cracking was not observed in microcapsules with $f_s \leq 0.5$. Imaging of the cross section of the membrane (Figure 5e) revealed that the membrane comprised a completely enclosed circular loop, which can be attributed to the enhanced rigidity of the capsules. The magnified TEM image of the membrane cross section exhibits a cylindrical PB phase embedded in a continuous PS phase, although the PB cylinders are short. The inset of Figure 5f shows a schematic diagram of a microcapsule with a cylindrical PB phase.

Phase Behavior of the Polymer Blend Confined in Spherical Membranes. The nanoscopic morphologies observed from the blends of block copolymer and *h*PS are summarized in a phase diagram in Figure 6, according to the weight fraction of PS. The addition of increasing quantities of *h*PS gives rise to morphological transitions from PS cylinders (C) to lamellae (L), PB cylinders (C), and PB spheres (S) by increasing the effective PS block ratio. Furthermore, an irregular bicontinuous phase (R) and perforated lamellae phase are produced in the compositional windows between the PS cylinder and the lamellae phases and between lamellae and PB cylinder phases, respectively. When the weight fraction of PS (f_s) is increased to 0.90, PB blocks form spherical domains, as shown in the last TEM image of Figure 6. The PB spheres are randomly distributed through the cross section, because the polymer blend contains only 15 wt % block copolymers for $f_s = 0.9$. On the other hand, the addition of *h*PS induces changes in the mechanical properties of the membrane. Although the microcapsules were rubbery and highly flexible in the absence of *h*PS, the membrane becomes rigid and brittle as the fraction of PS increases. For $f_s = 0.75$, the capsules show long cracks even under low bending, as shown in Figure S2 of the Supporting Information.

Conclusions

We have prepared microcapsules of triblock copolymers from water-in-oil-in-water (W/O/W) double emulsions and demonstrated the diverse nanostructures that such copolymers can form within the spherical shell of a microcapsule. A two-step emulsification method was used to prepare double-emulsion droplets composed of an aqueous core and a volatile oily middle phase containing the block copolymers. Next, the solvent molecules in the oil phase were slowly evaporated, yielding polymeric

microcapsules with a thin membrane. Single-cored microcapsules were then separated selectively, through spontaneous sedimentation, by controlling the densities of the core and the continuous phase. The internal morphology within the block copolymer shells could be modulated by adding *h*PS with relatively low molecular weight. Lamellae, perforated lamellae, and cylindrical and spherical phases were observed in the membrane of the capsules, depending on the weight fraction of PS in the block copolymer/*h*PS blend. Moreover, the addition of *h*PS could be used to control the mechanical characteristics of the microcapsules. The nanostructured membrane in the microcapsules is a promising template to make nanopores that connect inside and outside of the capsules. The one polymer block can be selectively removed from the membrane by various approaches including ozonation, self-degradation, or swelling-induced reconstruction.[11,33,34] Because the regular nanopores facilitate controlled mass transfer, our microcapsules have great potential in fields such as drug delivery and cosmetics, where they can be used for the encapsulation and controlled release of aqueous materials.

Experimental Section

Materials. Gelatin from porcine skin and polysaccharide (Ficoll PM 400) were purchased from Sigma. Symmetric SBS triblock copolymer (molecular weight of MW = 110 000 g/mol) was obtained from LG Chem. Polystyrene homopolymer (*h*PS) (MW = 2400 g/mol) was purchased from Aldrich. Dichloromethane (Aldrich) and toluene (Merck) were used as solvents for the polymers. A PEO-*b*-PPO-*b*-PEO triblock copolymer (Pluronic F108, BASF) was used as a surfactant. A 2 wt % aqueous solution of osmium tetraoxide (OsO_4, Polysciences) was used to selectively stain unsaturated blocks of the block copolymers for transmission electron microscopy (TEM) imaging. An epoxy resin (EpoFix kit, Struers) was used to prepare specimens for the cross-sectional TEM imaging.

Preparation of the Block Copolymer Microcapsules. As templates for block copolymer microcapsules, we used W/O/W double emulsion droplets, which were prepared by sequential emulsification. A 5 wt % polymer solution was prepared by dissolving SBS triblock copolymer and *h*PS in a mixture of dichloromethane and toluene. A 1-mL aliquot of 3.85 wt % aqueous gelatin solution was emulsified in 1 mL of polymer solution using a vortex mixer (Scientific Industries; Vortex−Genie2) for 1 min (first emulsification). To make double-emulsion droplets, a W/O-type emulsion droplet suspension was emulsified into 10 mL of a 0.1 wt % aqueous surfactant solution of Pluronic F108, using a homogenizer (Heidolph; DIAX900) at a speed of 12 000 rpm for 1 min (second emulsification). To evaporate the dichloromethane and toluene solvent molecules from the shell phase of the double-emulsion droplets, the droplet suspension was kept at 40 °C with gentle stirring for 1 h. The microcapsules then were washed with distilled water several times, to remove any residual surfactant through repeated centrifugation at 8500 rpm for 10 min, followed by redispersion in distilled water. The suspension was kept in an oven at 95 °C for 3 h to induce microphase separation of the block copolymers confined in the microcapsule membranes. A 10 or 20 w/v% aqueous Ficoll solution was also used as the core water phase of a W/O/W emulsion when a higher density of microcapsules was required in the separation process.

Density-Gradient Centrifugation. For polymer microcapsules with $f_s = 0.31$, fractionation was performed using a linear density gradient of Ficoll 400. A two-jar type gradient forming device (Sigma, G6897) was used to generate a 0−5 wt % linear gradient inside a glass tube; 1 mL of the microcapsule suspension was carefully loaded on top of 7 mL of the gradient solution. The solution then was ultracentrifuged using a swing-bucket rotor at an acceleration of 4500 *g* for 20 min. Each microcapsule settled until it reached the density-matched position, resulting in a broad distribution of microcapsules through the gradient solution.

Electron Microscopy. The microphases of the block copolymers confined in the membrane were investigated via TEM analysis. The microcapsule suspension was dropped onto a Formvar/carbon-coated TEM grid and dried completely. To obtain proper contrast between the PS and PB phases under TEM analysis, the PB phase was selectively stained with the vapor from a 2 wt % aqueous OsO_4 solution for 1 h. To observe the cross section of the membrane, on the other hand, the OsO_4-stained microcapsules were embedded in an epoxy resin and solidified at room temperature for 24 h. Ultrathin sections (50−70 nm) of the microcapsules were prepared at room temperature, using a diamond knife (Drukker) and an ultramicrotome (EM UC6, Leica), and mounted on a Formvar/carbon-coated TEM grid, using a loop. The prepared samples were examined in bright-field mode using a FE-TEM system (TECNAI G2 F30, FEI Company) and a FE-EF-TEM system (JEM 2200F, JEOL, Ltd.) operated at 200 kV.

Acknowledgment. We thank Prof. Paul Chaikin for valuable discussions. This work was supported by a grant from the Creative Research Initiative Program of the Ministry of Education, Science and Technology for "Complementary Hybridization of Optical and Fluidic Devices for Integrated Optofluidic Systems". The authors also appreciate partial support from the Brain Korea 21 Program. G.-R.Y. is thankful for the support by a NRF grant (No. 2009-0082451) funded by MEST.

Supporting Information Available: Optical microscopy and SEM images are included to show polydisperse microspheres produced by sequential emulsification and brittleness of microcapsules with high PS fraction, respectively. This material is available free of charge via the Internet at http://pubs.acs.org.

(33) Boudouris, B. W.; Frisbie, C. D.; Hillmyer, M. A. *Macromolecules* **2008**, *41*, 67–75.
(34) Wang, Y.; He, C.; Xing, W.; Li, F.; Tong, L.; Chen., Z.; Liao, X.; Steinhart, M. *Adv. Mater.* **2010**, *22*, 2068–2072.